Mathematics

Research article

Stability estimates for singularly perturbed Fisher's equation using element-free Galerkin algorithm

Jagbir Kaur and Vivek Sangwan[*]

School of Mathematics, Thapar Institute of Engineering & Technology, Patiala 147004, Punjab, India

* **Correspondence:** Email: sangwan.vivek@gmail.com.

Abstract: In the present article, a mesh-free technique has been presented to study the behavior of nonlinear singularly perturbed Fisher's problem, which exhibits the traveling wave propagation phenomenon. Some narrow regions adjacent to the left and right lateral boundary may possess rapid variations when the singular perturbation parameter $\epsilon \to 0$, which are not captured nicely by the traditional numerical schemes. In the current work, a robust numerical strategy is proposed, which comprises the implicit Crank-Nicolson scheme to discretize the time derivative term and the element-free Galerkin (EFG) scheme to discretize the spatial derivative terms with nodes densely distributed in the boundary layer regions. The stability of the semi-discrete scheme has been analyzed, and the rate of convergence is shown to be $O(\tau^2)$. The nonlinear nature of the considered problem has been tackled by employing the quasilinearization process, and its convergence rate has been discussed. Some numerical experiments have been performed to verify the computational uniformity and robustness of the suggested method, rate of convergence as well L_∞ errors have been presented, which depicts the effectiveness of the proposed method.

Keywords: singularly perturbed problems; nonlinear time-dependent Fisher equation; moving least-squares approximation; implicit Crank-Nicolson technique; element-free Galerkin scheme
Mathematics Subject Classification: 65L11, 65M12

1. Introduction

In 1937, Fisher [10] examined the contrast of linear diffusion and nonlinear reaction terms and proposed the Fisher equation as a model for the propagation of genes in a habitat with an advantageous selection intensity. The present study deals with one such kind of Eq (1.1) known as time-dependent singularly perturbed Fisher problem given by

$$\frac{\partial y(x,t)}{\partial t} = \epsilon \nabla^2 y(x,t) + \beta y(x,t)(1 - y(x,t)), \quad (x,t) \in \Omega \equiv \Omega_x \times \Omega_t \equiv (0,1) \times (0,T], \qquad (1.1)$$

with initial condition

$$y(x, 0) = y_0(x), \ x \in \bar{\Omega}_x, \tag{1.2}$$

and boundary conditions as

$$y(0, t) = f(t), \ y(1, t) = g(t), \ t \in \bar{\Omega}_t, \tag{1.3}$$

where $y(x, t)$ symbolizes the occurrence of traveling wave, the parameter β is non-negative and $\partial\Omega = \bar{\Omega}\backslash\Omega$ is the boundary of the domain. In Eq (1.1), ϵ is known as singular perturbation parameter satisfying $0 < \epsilon \ll 1$. The problem (1.1) becomes singularly perturbed in the case $\epsilon \to 0$. The considered Fisher's problem is widely encountered in chemical kinetics [11] and population dynamics [12] which include problems such as nonlinear evolution of a population in habitat, flame propagation in nuclear reactor theory, the branching Brownian motion process [6] etc. Due to the extensive range of applications, researchers have been interested in Fisher's problem's analytical and numerical solutions. Different analytical and numerical approaches have been developed to solve Fisher's equation.

Wazwaz and Gorguis [25] developed an analytical solution of generalized Fisher's equation by using the Adomian decomposition methodology. Rosa et al. [20] presented an application of Lie point symmetries for generalized Fisher equation modeling the tumor progression in biological interests. Analytical solutions have been obtained for the growth of tumors at their interfaces which represent motility through white and gray matter in the brain. A numerical analysis of the reaction-diffusion problem has been carried out by Al-Khaled [2] by employing the sinc collection approach. Ablowitz and Zeppetella [1] derived an explicit solution of the traveling wave equation and determined the exact solution for a particular value of wave speed $c = 5/\sqrt{6}$. Thenceforth, Wang [24] obtained exact and explicit solitary wave solutions of generalized Fisher's equation by introducing a mathematical method based on the nonlinear transformation. Analytical representations of various traveling wave solutions for the Fisher's equation have been derived by Brazhnik and Tyson [22] in two spatial dimensions. Feng and Li [9] obtained complex traveling wave solutions by reducing Fisher's equation to a first-order integrable ordinary differential equation using the first integral method. Mittal and Jiwari [17] adopted the differential quadrature method to study the numerical solutions of Fisher's equation. A pseudospectral technique was presented by Olmos and Shizgal [18], later by Balyan et al. [4]. Carey and Shen [7] developed a least-squares finite-element formulation for solving Fisher's equation. Petrov-Galerkin finite element method has been presented by Tang and Weber [21] to deal with Fisher's problem. Khader and Saad [13] developed a numerical technique for solving the fractional Fisher equation, which represents the problem of biological invasion. The spectral collocation technique based upon Chebyshev approximations was employed to reduce the considered problem into a system of ordinary differential equations, which were further solved by the finite difference method. Radial basis functions based meshfree approach for solving extended Fisher-Kolmogorov model was studied by Kumar et al. [14]. Mickens [16] formulated a finite-difference scheme according to the nonstandard modeling rules to deal with Fisher's equation. Atangana [3] applied fractional derivatives, introduced by Caputo and Fabrizio, to the nonlinear Fisher's equation and derived a unique solution using the Sumudu decomposition iterative method.

Even though Fisher's problem has vast applications in diverse areas of science and engineering, only a few researchers have paid attention to the solution strategies for Fisher's problem. More precisely,

in the singularly perturbed case of the problem, i.e., for $\epsilon \ll 1$, hardly any researcher has proposed any numerical scheme so far. Dag and Ersoy [8] suggested a collocation scheme for solving Fisher's equation with a small value of the diffusion coefficient ϵ. Full discretization of the problem is achieved by employing the Crank-Nicolson method in time and the exponential B-spline process in a spatial variable. Uzunca et al. [23] developed a discontinuous Galerkin approach with a moving mesh strategy for solving nonlinear Fisher's equation with traveling wave solutions. Numerical results demonstrate different natures of traveling waves for $\epsilon \to 0$.

Since the conventional numerical techniques are not perfectly capable of approximating the solutions of singularly perturbed problems (SPPs) in the boundary layer region due to the singularly perturbed nature of the problem, we need to follow some specific approach to capture these boundary layers when $\epsilon \to 0$. The primary goal of this work is to provide a robust and efficient numerical strategy known as the element-free Galerkin (EFG) technique [15, 26] for capturing the sharpness of solutions. So far, no mesh-free methods have been employed to solve singularly perturbed Fisher's equation. The non-requirement of node connectivity is a vital feature of the proposed technique, due to which node particles can be added or deleted without any difficulty. As a result, rapid and effective refining of domain discretization can be achieved. Non-uniformly distributed nodes that condense in the boundary layer area have been developed in the paper to accomplish this advantage. This feature makes the EFG technique more adaptive than the finite element method (FEM), particularly for SPPs. On the other hand, the EFG technique has a few downsides compared to FEM. The EFG procedure is computationally expensive than the FEM method and has a more complicated implementation algorithm. The proposed scheme employs the moving least squares (MLS) approximation for generating shape functions. The methodology is based on the global weak form, and the numerical integrations are computed by employing the Gauss quadrature background cells. The implicit Crank-Nicolson method has been used to discretization the time derivative before the spatial discretization. The quasilinearization process proposed by Bellman and Kalaba [5] has been invoked to deal with the nonlinearity existing in the problem. Since the MLS shape functions do not fulfill the Kronecker delta function property, the Lagrange multipliers method is utilized to impose the essential boundary conditions.

The work presented in the paper is organized as follows. The temporal discretizaton using Crank-Nicolson scheme has been discussed in Section 2. Stability and convergence of the time discrete approach have been investigated in Section 3. Section 4 deals with the quasilinearization process and its rate of convergence. The EFG approach has been discussed in detail in Section 5. Section 6 contains the numerical examples followed by conclusion and bibliography.

2. Time semi-discretization

2.1. Notations and preliminaries

In this subsection, we define the functional spaces along with the standard norms and inner products which have been utilized in the next Sections.

Consider the H^1-space defined by

$$H^1(\Omega) = \{\vartheta \in L^2(\Omega), \nabla\vartheta \in L^2(\Omega)\},$$
$$H^1_0(\Omega) = \{\vartheta \in H^1(\Omega), \vartheta|_{\partial\Omega} = 0\},$$

where $\nabla\vartheta = \frac{\partial\vartheta}{\partial x}$ and $L^2(\Omega)$ is the space of all square integrable functions in Ω. The inner product of $L^2(\Omega)$ and $H^1(\Omega)$ are defined respectively as

$$< \vartheta, \xi >= \int_\Omega \vartheta\xi d\Omega, < \vartheta, \xi >_1 =< \vartheta, \xi > + < \nabla\vartheta, \nabla\xi > .$$

The L^2- and H^1-norms are defined respectively as

$$\|\vartheta\| =< \vartheta, \vartheta >^{1/2}, \quad \|\vartheta\|_1 =< \vartheta, \vartheta >_1^{1/2}, \quad |\vartheta|_1 =< \nabla\vartheta, \nabla\vartheta >^{1/2} .$$

2.2. Semi-discrete scheme

We define $t_n = n\tau$, $n = 0, 1, ..., N$, where $\tau = T/N$ is the step-size of the time variable. Next, we discretize the time derivative with implicit Crank-Nicolson scheme for problem (1.1) as follows

$$\frac{y^{(n+1)} - y^{(n)}}{\tau} = \epsilon\frac{\nabla^2 y^{(n+1)} + \nabla^2 y^{(n)}}{2} + \beta\frac{y^{(n+1)} + y^{(n)}}{2} - \beta\frac{(y^2)^{(n+1)} + (y^2)^{(n)}}{2}, \quad n = 0, 1, ..., N, \qquad (2.1)$$

where $\nabla^2 y^{(n+1)} = \frac{\partial^2 y^{(n+1)}}{\partial x^2}$. Simplifying equation (2.1) results in

$$y^{(n+1)} - \frac{\tau\epsilon}{2}\nabla^2 y^{(n+1)} - \frac{\tau\beta}{2}y^{(n+1)} + \frac{\tau\beta}{2}(y^2)^{n+1} = y^{(n)} + \frac{\tau\epsilon}{2}\nabla^2 y^{(n)} + \frac{\tau\beta}{2}y^{(n)} - \frac{\tau\beta}{2}(y^2)^{(n)}, \qquad (2.2)$$

where $y^{(n+1)}$ is the solution of the above differential equation (2.2) at $(n + 1)^{th}$ time level.

3. Stability and convergence of the time-discrete scheme

Lemma 3.1. *Let $y \in C(\overline{\Omega})$ and $\overline{\Omega} \subset \mathbb{R}^2$ be a bounded closed set. Then the polynomial function $F(y)$ satisfies the inequality*

$$|F(y)| \le \overline{M}.$$

Proof. According to the assumption, we have $\min\{y : y \in C(\overline{\Omega})\} \le y \le \max\{y : y \in C(\overline{\Omega})\}$, and thus $\exists$ a positive integer M such that

$$\max_{y\in C(\overline{\Omega})} |y| \le M.$$

This proves the result. $\qquad\qquad\qquad\square$

Theorem 3.1. *Suppose $y^{(n+1)} \in H^1(\overline{\Omega})$. Then the time discrete scheme (2.2) is unconditionally stable.*

Proof. The variational weak formulation of Eq (2.2) is given by

$$< y^{(n+1)}, \upsilon > + \frac{\tau\epsilon}{2} < \nabla y^{(n+1)}, \nabla\upsilon > - \frac{\tau\beta}{2} < y^{(n+1)}, \upsilon > + \frac{\tau\beta}{2} < (y^2)^{(n+1)}, \upsilon >=< y^{(n)}, \upsilon >$$

$$- \frac{\tau\epsilon}{2} < \nabla y^{(n)}, \nabla\upsilon > + \frac{\tau\beta}{2} < y^{(n)}, \upsilon > - \frac{\tau\beta}{2} < (y^2)^{(n)}, \upsilon >, \quad \forall\upsilon \in H^1(\Omega) \qquad (3.1)$$

Setting $\upsilon = y^{(n+1)}$ in above Eq (3.1) yields

$$< y^{(n+1)}, y^{(n+1)} > + \frac{\tau\epsilon}{2} < \nabla y^{(n+1)}, \nabla y^{(n+1)} > - \frac{\tau\beta}{2} < y^{(n+1)}, y^{(n+1)} > + \frac{\tau\beta}{2} < (y^2)^{(n+1)}, y^{(n+1)} >$$

$$= < y^n, y^{(n+1)} > - \frac{\tau\epsilon}{2} < \nabla y^{(n)}, \nabla y^{(n+1)} > + \frac{\tau\beta}{2} < y^{(n)}, y^{(n+1)} > - \frac{\tau\beta}{2} < (y^2)^{(n)}, y^{(n+1)} > . \tag{3.2}$$

Taking L^2-norm over Ω and using the Cauchy-Schwarz inequality, we get

$$\left\|y^{(n+1)}\right\|_{L^2(\Omega)}^2 + \frac{\tau\epsilon}{2}\left\|\nabla y^{(n+1)}\right\|_{L^2(\Omega)}^2 - \frac{\tau\beta}{2}\left\|y^{(n+1)}\right\|_{L^2(\Omega)}^2 \le \left\|y^{(n)}\right\|_{L^2(\Omega)}\cdot\left\|y^{(n+1)}\right\|_{L^2(\Omega)} + \frac{\tau\epsilon}{2}\left\|\nabla y^{(n)}\right\|_{L^2(\Omega)}\cdot\left\|\nabla y^{(n+1)}\right\|_{L^2(\Omega)}$$

$$+ \frac{\tau\beta}{2}\left\|y^{(n)}\right\|_{L^2(\Omega)}\cdot\left\|y^{(n+1)}\right\|_{L^2(\Omega)} + \frac{\tau\beta}{2}\left\|(y^2)^{(n+1)}\right\|_{L^2(\Omega)}\cdot\left\|y^{(n+1)}\right\|_{L^2(\Omega)}$$

$$+ \frac{\tau\beta}{2}\left\|(y^2)^{(n)}\right\|_{L^2(\Omega)}\cdot\left\|y^{(n+1)}\right\|_{L^2(\Omega)}. \tag{3.3}$$

Taking F(y)=y and utilizing the Lemma 3.1 outputs

$$\left\|y^{(n+1)}\right\|_{L^2(\Omega)}^2 + \frac{\tau\epsilon}{2}\left\|\nabla y^{(n+1)}\right\|_{L^2(\Omega)}^2 - \frac{\tau\beta}{2}\left\|y^{(n+1)}\right\|_{L^2(\Omega)}^2 \le \left\|y^{(n)}\right\|_{L^2(\Omega)}\left\|y^{(n+1)}\right\|_{L^2(\Omega)} + \frac{\tau\epsilon}{2}\left\|\nabla y^{(n)}\right\|_{L^2(\Omega)}\left\|\nabla y^{(n+1)}\right\|_{L^2(\Omega)}$$

$$+ \frac{\tau\beta}{2}\left\|y^{(n)}\right\|_{L^2(\Omega)}\left\|y^{(n+1)}\right\|_{L^2(\Omega)} + \frac{\tau\beta}{2}\overline{M}\left\|y^{(n+1)}\right\|_{L^2(\Omega)}^2$$

$$+ \frac{\tau\beta}{2}\overline{M}\left\|y^{(n)}\right\|_{L^2(\Omega)}\left\|y^{(n+1)}\right\|_{L^2(\Omega)}.$$

Simplifying the above relation, we get

$$\frac{1}{2}\left\|y^{(n+1)}\right\|_{L^2(\Omega)}^2 + \frac{\tau\epsilon}{4}\left\|\nabla y^{(n+1)}\right\|_{L^2(\Omega)}^2 \le \frac{1}{2}\left\|y^{(n)}\right\|_{L^2(\Omega)}^2 + \frac{\tau\epsilon}{4}\left\|\nabla y^{(n)}\right\|_{L^2(\Omega)}^2 + (1+\overline{M})\frac{\tau\beta}{4}\left\|y^{(n)}\right\|_{L^2(\Omega)}^2$$

$$+ (1+\overline{M})\frac{3\tau\beta}{4}\left\|y^{(n+1)}\right\|_{L^2(\Omega)}^2. \tag{3.4}$$

Next, we define the following weighted Hilbert norm

$$\left\|y^{(n+1)}\right\|_{H_w(\Omega)}^2 = \frac{1}{2}\left\|y^{(n+1)}\right\|_{L^2(\Omega)}^2 + \frac{\tau\epsilon}{4}\left\|\nabla y^{(n+1)}\right\|_{L^2(\Omega)}^2.$$

Then Eq (3.4) can be rewritten as

$$\left\|y^{(n+1)}\right\|_{H_w(\Omega)}^2 \le \left\|y^{(n)}\right\|_{H_w(\Omega)}^2 + (1+\overline{M})\frac{\tau\beta}{4}\left\|y^{(n)}\right\|_{H_w(\Omega)}^2 + (1+\overline{M})\frac{3\tau\beta}{4}\left\|y^{(n+1)}\right\|_{H_w(\Omega)}^2. \tag{3.5}$$

Taking summation for i from 0 to $n-1$,

$$\sum_{i=0}^{n-1}\left\|y^{(i+1)}\right\|_{H_w(\Omega)}^2 \le \sum_{i=0}^{n-1}\left\|y^{(i)}\right\|_{H_w(\Omega)}^2 + (1+\overline{M})\frac{\tau\beta}{4}\sum_{i=0}^{n-1}\left\|y^{(i)}\right\|_{H_w(\Omega)}^2 + (1+\overline{M})\frac{3\tau\beta}{4}\sum_{i=0}^{n-1}\left\|y^{(i+1)}\right\|_{H_w(\Omega)}^2,$$

or equivalently

$$\left\|y^{(n)}\right\|_{H_w(\Omega)}^2 \le \left\|y^{(0)}\right\|_{H_w(\Omega)}^2 + (1+\overline{M})\tau\beta\sum_{i=0}^{n-1}\left\|y^{(i+1)}\right\|_{H_w(\Omega)}^2.$$

Using Gronwall lemma, we get

$$\left\|y^{(n)}\right\|^2_{H_w(\Omega)} \le \left\|y^{(0)}\right\|^2_{H_w(\Omega)} \exp\left((1 + \overline{M})n\tau\beta\right)$$

$$\le \left\|y^{(0)}\right\|^2_{H_w(\Omega)} \exp\left((1 + \overline{M})T\beta\right)$$

$$\le C\left\|y^{(0)}\right\|^2_{H_w(\Omega)}.$$

Thus, the numerical scheme (2.2) is unconditionally stable. □

Theorem 3.2. *The discrete scheme* (2.2) *is convergent with order of convergence* $O(\tau^2)$.

Proof. Let $y^{(n)}$ and $Y^{(n)}$ be the exact and computed solutions of the temporal discrete scheme (2.2) respectively.

Then, we have

$$< y^{(n+1)}, \upsilon > + \frac{\tau\epsilon}{2} < \nabla y^{(n+1)}, \nabla\upsilon > -\frac{\tau\beta}{2} < y^{(n+1)}, \upsilon > +\frac{\tau\beta}{2} < (y^2)^{(n+1)}, \upsilon >=< y^{(n)}, \upsilon >$$

$$-\frac{\tau\epsilon}{2} < \nabla y^{(n)}, \nabla\upsilon > +\frac{\tau\beta}{2} < y^{(n)}, \upsilon > -\frac{\tau\beta}{2} < (y^2)^{(n)}, \upsilon > +\tau < R_\tau, \upsilon >, \qquad (3.6)$$

where the residual R satisfies $|R_\tau| \le C\tau^2$ and C is a positive constant.

Since $Y^{(n)}$ is approximate solution, hence

$$< Y^{(n+1)}, \upsilon > + \frac{\tau\epsilon}{2} < \nabla Y^{(n+1)}, \nabla\upsilon > -\frac{\tau\beta}{2} < Y^{(n+1)}, \upsilon > +\frac{\tau\beta}{2} < (Y^2)^{(n+1)}, \upsilon >=< Y^{(n)}, \upsilon >$$

$$-\frac{\tau\epsilon}{2} < \nabla Y^{(n)}, \nabla\upsilon > +\frac{\tau\beta}{2} < Y^{(n)}, \upsilon > -\frac{\tau\beta}{2} < (Y^2)^{(n)}, \upsilon > . \qquad (3.7)$$

Subtracting Eq (3.7) from Eq (3.6) results in

$$< \mathfrak{L}^{(n+1)}, \upsilon > + \frac{\tau\epsilon}{2} < \nabla\mathfrak{L}^{(n+1)}, \nabla\upsilon > -\frac{\tau\beta}{2} < \mathfrak{L}^{(n+1)}, \upsilon > +\frac{\tau\beta}{2} < (y^2)^{(n+1)} - (Y^2)^{(n+1)}, \upsilon >$$

$$=< \mathfrak{L}^{(n)}, \upsilon > -\frac{\tau\epsilon}{2} < \nabla\mathfrak{L}^{(n)}, \nabla\upsilon > +\frac{\tau\beta}{2} < \mathfrak{L}^{(n)}, \upsilon > -\frac{\tau\beta}{2} < (y^2)^{(n)} - (Y^2)^{(n)}, \upsilon >$$

$$+\tau < R_\tau, \upsilon >,$$

where, $\mathfrak{L}^{(n)} = y^{(n)} - Y^{(n)}, n \ge 1, \mathfrak{L}^{(0)} = 0.$

Setting $\upsilon = \mathfrak{L}^{(n+1)}$, we have

$$< \mathfrak{L}^{(n+1)}, \mathfrak{L}^{(n+1)} > + \frac{\tau\epsilon}{2} < \nabla\mathfrak{L}^{(n+1)}, \nabla\mathfrak{L}^{(n+1)} > -\frac{\tau\beta}{2} < \mathfrak{L}^{(n+1)}, \mathfrak{L}^{(n+1)} >=< \mathfrak{L}^{(n)}, \mathfrak{L}^{(n+1)} > -\frac{\tau\epsilon}{2} < \nabla\mathfrak{L}^{(n)}, \nabla\mathfrak{L}^{(n+1)} >$$

$$+ \frac{\tau\beta}{2} < \mathfrak{L}^{(n)}, \mathfrak{L}^{(n+1)} > -\frac{\tau\beta}{2} < (y^2)^{(n+1)} - (Y^2)^{(n+1)}, \mathfrak{L}^{(n+1)} >$$

$$-\frac{\tau\beta}{2} < (y^2)^{(n)} - (Y^2)^{(n)}, \mathfrak{L}^{(n+1)} > +\tau < R_\tau, \mathfrak{L}^{(n+1)} > .$$

Now employing Lipschitz condition Cauchy-Schwarz inequality, we obtain

$$\left\|\mathfrak{L}^{(n+1)}\right\|^2_{L^2(\Omega)} + \frac{\tau\epsilon}{2}\left\|\nabla\mathfrak{L}^{(n+1)}\right\|^2_{L^2(\Omega)} - \frac{\tau\beta}{2}\left\|\mathfrak{L}^{(n+1)}\right\|^2_{L^2(\Omega)}$$

$$\leq \left\|\mathfrak{L}^{(n)}\right\|_{L^2(\Omega)}\left\|\mathfrak{L}^{(n+1)}\right\|_{L^2(\Omega)} + \frac{\tau\epsilon}{2}\left\|\nabla\mathfrak{L}^{(n)}\right\|_{L^2(\Omega)}\left\|\nabla\mathfrak{L}^{(n+1)}\right\|_{L^2(\Omega)}$$

$$+\frac{\tau\beta}{2}\left\|\mathfrak{L}^{(n)}\right\|_{L^2(\Omega)}\left\|\mathfrak{L}^{(n+1)}\right\|_{L^2(\Omega)} + \frac{\tau\beta}{2}C^*\left\|y^{(n+1)} - Y^{(n+1)}\right\|_{L^2(\Omega)}\left\|\mathfrak{L}^{(n+1)}\right\|_{L^2(\Omega)}$$

$$+\frac{\tau\beta}{2}C^*\left\|y^{(n)} - Y^{(n)}\right\|_{L^2(\Omega)}\left\|\mathfrak{L}^{(n+1)}\right\|_{L^2(\Omega)} + \tau\left\|R_\tau\right\|_{L^2(\Omega)}\left\|\mathfrak{L}^{(n+1)}\right\|_{L^2(\Omega)}.$$

Simplifying further, we get

$$\frac{1}{2}\left\|\mathfrak{L}^{(n+1)}\right\|_{L^2(\Omega)}^2 + \frac{\tau\epsilon}{4}\left\|\nabla\mathfrak{L}^{(n+1)}\right\|_{L^2(\Omega)}^2 \leq \frac{1}{2}\left\|\mathfrak{L}^{(n)}\right\|_{L^2(\Omega)}^2 + \frac{\tau\epsilon}{4}\left\|\nabla\mathfrak{L}^{(n)}\right\|_{L^2(\Omega)}^2 + ((1+C^*)\frac{3\beta}{4} + \frac{1}{2})\tau\left\|\mathfrak{L}^{(n+1)}\right\|_{L^2(\Omega)}^2$$

$$+ (1+C^*)\frac{\tau\beta}{4}\left\|\mathfrak{L}^{(n)}\right\|_{L^2(\Omega)}^2 + \frac{\tau}{2}\left\|R_\tau\right\|_{L^2(\Omega)}^2. \tag{3.8}$$

By defining the following weighted Hilbert norm

$$\left\|\mathfrak{L}^{(n+1)}\right\|_{H_w(\Omega)}^2 = \frac{1}{2}\left\|\mathfrak{L}^{(n+1)}\right\|_{L^2(\Omega)}^2 + \frac{\tau\epsilon}{4}\left\|\nabla\mathfrak{L}^{(n+1)}\right\|_{L^2(\Omega)}^2.$$

Equation (3.8) can be rewritten as

$$\left\|\mathfrak{L}^{(n+1)}\right\|_{H_w(\Omega)}^2 \leq \left\|\mathfrak{L}^{(n)}\right\|_{H_w(\Omega)}^2 + ((1+C^*)\frac{3\beta}{4} + \frac{1}{2})\tau\left\|\mathfrak{L}^{(n+1)}\right\|_{H_w(\Omega)}^2 + (1+C^*)\frac{\tau\beta}{4}\left\|\mathfrak{L}^{(n)}\right\|_{H_w(\Omega)}^2 + \frac{\tau}{2}\left\|R_\tau\right\|_{L^2(\Omega)}^2.$$

Taking summation for i from 0 to $n-1$,

$$\sum_{i=0}^{n-1}\left\|\mathfrak{L}^{(i+1)}\right\|_{H_w(\Omega)}^2 \leq \sum_{i=0}^{n-1}\left\|\mathfrak{L}^{(i)}\right\|_{H_w(\Omega)}^2 + \left((1+C^*)\beta + \frac{1}{2}\right)\tau\sum_{i=0}^{n}\left\|\mathfrak{L}^{(i+1)}\right\|_{H_w(\Omega)}^2 + \frac{n\tau}{2}\left\|R_\tau\right\|_{L^2(\Omega)}^2.$$

Using Gronwall lemma, we get

$$\left\|\mathfrak{L}^{(n)}\right\|_{H_w(\Omega)}^2 \leq \left[\left\|\mathfrak{L}^{(0)}\right\|_{H_w(\Omega)}^2 + \frac{n\tau}{2}\left\|R_\tau\right\|_{L^2(\Omega)}^2\right]\exp\left(((1+C^*)\beta + \frac{1}{2})n\tau\right) \tag{3.9}$$

$$\leq \left[\frac{T}{2}\left\|R_\tau\right\|_{L^2(\Omega)}^2\right]\exp\left(C^{**}T\right) \tag{3.10}$$

$$\leq \mathbf{C(T)}\left\|R_\tau\right\|_{L^2(\Omega)}^2 \tag{3.11}$$

$$\leq \mathbf{C(T)}\tau^4. \tag{3.12}$$

Thus we have

$$\left\|\mathfrak{L}^{(n)}\right\|_{H_w(\Omega)} \leq \mathbf{C(T)}\tau^2,$$

which completes the proof. □

4. Quasilinearization technique

As the problem under consideration is nonlinear in nature, and quasilinearization is a standard technique broadly used for approximating the nonlinear problems by their linearized version

for obtaining the approximate solutions, in this Section, we will linearize Eq (2.2) using the quasilinearization process and will discuss its convergence.

Using the quasilinearization process by Bellman and Kalaba [5], Eq (2.2) can be linearized as follows:

$$-\epsilon\frac{\tau}{2}\nabla^2 y^{(n+1),(k+1)} + [1 - \beta\frac{\tau}{2} + \beta\tau y^{(n+1),(k)}]y^{(n+1),(k+1)} \tag{4.1}$$
$$= (1 + \beta\frac{\tau}{2})y^{(n)} + \epsilon\frac{\tau}{2}\nabla^2 y^{(n)} - \beta\frac{\tau}{2}(y^2)^{(n)} + \beta\frac{\tau}{2}(y^2)^{(n+1),(k)},$$

with initial condition $y^{(0),(k+1)} = y_0(x)$, and boundary conditions

$$y^{(n+1),(k+1)}(0,t) = f(t^{(n+1)}) \ \ and \ \ y^{(n+1),(k+1)}(1,t) = g(t^{(n+1)}), \tag{4.2}$$

where $y^{(n+1),(k+1)}$ denotes the approximate solution at time level $(n + 1)^{th}$ and $(k + 1)^{th}$ iteration.

Theorem 4.1. *(Convergence of quasilinearization technique) Let $\{y^{(n+1),(k)}\}_{k=0}^\infty$ be the sequence produced by quasilinearization technique at $(n + 1)^{th}$ time level and $(k)^{th}$ iteration. Then there exist a constant $Q > 0$, independent of n, such that*

$$\|y^{(n+1),(k+1)} - y^{(n+1),(k)}\|_{\bar{\Omega}_x} \le Q\|y^{(n+1),(k)} - y^{(n+1),(k-1)}\|^2_{\bar{\Omega}_x}, \tag{4.3}$$

i.e., the quasilinearization process converges quadratically.

Proof. In order to prove the convergence of the quasilinearization process, we consider

$$\epsilon\nabla^2 y^{(n+1)} = F(y^{n+1}), \ \ x \in \Omega_x, \ \ n \ge 0,$$
$$y^{(n+1)}(0,t) = f(t^{n+1}), \ \ y^{(n+1)}(1,t) = g(t^{n+1}), \ \ n \ge 0.$$

We assume $y^{(n+1),(k=0)}$ be the initial guess which also incorporates the boundary conditions.

By applying quasilinearization process, we obtain a sequence $\{y^{(n+1),(k)}\}_{k=0}^\infty$ of linear differential equations determined by the following recurrence relation:

$$\epsilon\nabla^2 y^{(n+1),(k+1)} \approx F(y^{(n+1),(k)}) + (y^{(n+1),(k+1)} - y^{(n+1),(k)})\frac{\partial F(y^{(n+1),(k)})}{\partial y}, \ \ x \in \Omega_x, \ \ n \ge 0, \tag{4.4}$$

$$y^{(n+1),(k+1)}(0,t) = f(t^{n+1}), \ \ y^{(n+1),(k+1)}(1,t) = g(t^{n+1}), \ \ x \in \Omega_x, \ \ n \ge 0.$$

Rewriting the above relation at the previous iteration step, we get

$$\epsilon\nabla^2 y^{(n+1),(k)} = F(y^{(n+1),(k-1)}) + (y^{(n+1),(k)} - y^{(n+1),(k-1)})\frac{\partial F(y^{(n+1),(k-1)})}{\partial y}, \ \ x \in \Omega_x, \ \ n \ge 0. \tag{4.5}$$

Subtracting Eq (4.5) from (4.4), we have

$$\epsilon(\nabla^2 y^{(n+1),(k+1)} - \nabla^2 y^{(n+1),(k)}) = F(y^{(n+1),(k)}) - F(y^{(n+1),(k-1)}) + (y^{(n+1),(k+1)} - y^{(n+1),(k)})\frac{\partial F(y^{(n+1),(k)})}{\partial y}$$

$$- (y^{(n+1),(k)} - y^{(n+1),(k-1)})\frac{\partial F(y^{(n+1),(k-1)})}{\partial y}, \ \ x \in \Omega_x, \ \ n \ge 0. \tag{4.6}$$

The above differential equation is of second order in terms of $(y^{(n+1),(k+1)} - y^{(n+1),(k)})$. With the help of Green's function, Eq (4.6) can be converted into an integral equation as

$$
\begin{aligned}
\epsilon(y^{(n+1),(k+1)} &- y^{(n+1),(k)}) \\
&= \int_0^1 G(x,s)\Big[F(y^{(n+1),(k)}) - F(y^{(n+1),(k-1)}) + (y^{(n+1),(k+1)} - y^{(n+1),(k)})\frac{\partial F(y^{(n+1),(k)})}{\partial y} \\
&\quad - (y^{(n+1),(k)} - y^{(n+1),(k-1)})\frac{\partial F(y^{(n+1),(k-1)})}{\partial y}\Big] ds, \quad x \in \Omega_x, \ \ n \geq 0,
\end{aligned}
\tag{4.7}
$$

where the Green's function $G(x,s)$ is defined by

$$
G(x,s) = \begin{cases} x(s-1), & 0 \leq x \leq s \leq 1, \\ (x-1)s, & 0 \leq s \leq x \leq 1, \end{cases}
$$

and

$$
\max_{x,s} G(x,s) = \frac{1}{4}.
\tag{4.8}
$$

Using mean-value theorem, we have

$$
\begin{aligned}
F(y^{(n+1),(k)}) - F(y^{(n+1),(k-1)}) &= (y^{(n+1),(k)} - y^{(n+1),(k-1)})\frac{\partial F(y^{(n+1),(k-1)})}{\partial y} \\
&\quad + \frac{(y^{(n+1),(k)} - y^{(n+1),(k-1)})^2}{2}\frac{\partial^2 F(\theta)}{\partial y^2},
\end{aligned}
\tag{4.9}
$$

where $y^{(n+1),(k-1)} \leq \theta \leq y^{(n+1),(k)}$. Now substituting the value of $F(y^{(n+1),(k)}) - F(y^{(n+1),(k-1)})$, in Eq (4.7), we get the following expression

$$
\epsilon(y^{(n+1),(k+1)} - y^{(n+1),(k)}) =
\tag{4.10}
$$
$$
\int_0^1 G(x,s)\Big[\frac{(y^{(n+1),(k)} - y^{(n+1),(k-1)})^2}{2}\frac{\partial^2 F(\theta)}{\partial y^2} + (y^{(n+1),(k+1)} - y^{(n+1),(k)})\frac{\partial F(y^{(n+1),(k)})}{\partial y}\Big] ds, \quad x \in \Omega_x, \ \ n \geq 0.
$$

Assume that

$$
\max_{|\theta| \leq 1}\left|\frac{\partial^2 F(\theta)}{\partial y^2}\right| = L, \quad \max_{|y^{(n+1),(k)}| \leq 1}\left|\frac{\partial F(y^{(n+1),(k)})}{\partial y}\right| = R.
\tag{4.11}
$$

Now using Eqs (4.8) and (4.11) in Eq (4.10) and taking maximum norm, we get

$$
\epsilon\left\|y^{(n+1),(k+1)} - y^{(n+1),(k)}\right\|_{\overline{\Omega}_x} \leq \frac{1}{4}\int_0^1 \Big[\frac{L}{2}(y^{(n+1),(k)} - y^{(n+1),(k-1)})^2 + R\left\|y^{(n+1),(k+1)} - y^{(n+1),(k)}\right\|_{\overline{\Omega}_x}\Big] ds.
$$

On simplifying this inequality, we get

$$
\begin{aligned}
\left\|(y^{(n+1),(k+1)} - y^{(n+1),(k)})\right\|_{\bar{\Omega}_x} &\leq \frac{L}{8\epsilon - 2R}\left\|(y^{(n+1),(k)} - y^{(n+1),(k-1)})\right\|^2_{\bar{\Omega}_x}, \\
&= Q\left\|(y^{(n+1),(k)} - y^{(n+1),(k-1)})\right\|^2_{\bar{\Omega}_x},
\end{aligned}
$$

where $Q = L/(8\epsilon - 2R)$.

Hence, with the appropriate choice of initial iterative approximation $y^{(n+1),(k=0)}$, the quasilinearization technique converges quadratically. $\square$

In Liu of the above theorem, in order to find the solution of the nonlinear problem (1.1), it is sufficient to find the solution of its approximate linearized problem (4.1). Following that, we will examine the proposed numerical scheme to approximate the solution to the linearized problem (4.1).

5. Element-free Galerkin formulation

Next, we will explain the element-free Galerkin formulation in detail.

5.1. Moving least squares approximation

Let $\Omega_h = \{\mathfrak{x}_i\}_{i=1}^n$ be distribution of nodes in the spatial domain $\Omega_x = [0, 1]$. Then the domain of influence of any typical node $\mathfrak{x}$ with radius $\mathfrak{d}_s$ is expressed as

$$\mathfrak{d}(\mathfrak{x}) = \{\mathfrak{x}^* \in \Omega_h : |\mathfrak{x} - \mathfrak{x}^*| < \mathfrak{d}_s(\mathfrak{x})\}.$$

So, the domain of influence for $\mathfrak{x}_i$ is given by

$$\mathfrak{d}_i = \{\mathfrak{x}^* \in \Omega_h : |\mathfrak{x}_i - \mathfrak{x}^*| < \mathfrak{d}_{si}\}.$$

We define the Gaussian exponential spline weight functions corresponding to node $\mathfrak{x}_i$ based on a normalized distance $s = \frac{|\mathfrak{x} - \mathfrak{x}_i|}{\mathfrak{d}_{si}}$ as

$$w_i(s) = \begin{cases} \frac{e^{-(s/\alpha)^2} - e^{-(1/\alpha)^2}}{1 - e^{-(1/\alpha)^2}}, & s < 1 \\ 0, & s \geq 1, \end{cases}$$

for $i = 1, 2, ..., n$. The employed weight functions $w_i(s)$ in MLS approximation must be monotonic decreasing, continuous and positive in the corresponding domain $\mathfrak{d}_i$. We define

$$\mathfrak{p}(\mathfrak{x}) = \left[\mathfrak{p}(\mathfrak{x}_1), \mathfrak{p}(\mathfrak{x}_2), ..., \mathfrak{p}(\mathfrak{x}_m)\right]^T, \mathfrak{x} \in \Omega_x,$$

as a set of polynomial basis functions. In the present work, we have used quadratic basis functions defined as

$$\mathfrak{p}(\mathfrak{x}) = [1, x, x^2].$$

Let the field function $y(\mathfrak{x})$ be approximated by $y_h(\mathfrak{x})$ using MLS approximation in the domain Ω where y_h is defined as

$$y_h(\mathfrak{x}) = \sum_{i=1}^m \mathfrak{p}_i(\mathfrak{x})\mathfrak{a}_i(\mathfrak{x}) = \mathfrak{p}^T(\mathfrak{x})\mathfrak{a}(\mathfrak{x}), \tag{5.1}$$

and $\mathfrak{a}$ is an unknown vector of coefficients determined by minimizing the weighted residual functional

$$J(\mathfrak{x}) = \sum_{i=1}^n w(\mathfrak{x} - \mathfrak{x}_i)\left[y(\mathfrak{x}_i) - \sum_{i=1}^m \mathfrak{p}_i(\mathfrak{x})\mathfrak{a}_i(\mathfrak{x})\right]^T.$$

The minimization of J with respect to $\mathfrak{a}(\mathfrak{x})$ leads to $\frac{\partial J}{\partial \mathfrak{a}} = 0$. This gives

$$\mathfrak{a}(\mathfrak{x}) = \mathbf{P}^{-1}(\mathfrak{x})\mathbf{S}(\mathfrak{x})\mathbf{y}, \tag{5.2}$$

where

$$\mathbf{P}(\mathfrak{x}) = \sum_{i=1}^{n} w(\mathfrak{x} - \mathfrak{x}_i)\mathfrak{p}(\mathfrak{x}_i)\mathfrak{p}^T(\mathfrak{x}_i),$$

$$\mathbf{S}(\mathfrak{x}) = \left[w(\mathfrak{x} - \mathfrak{x}_1)\mathfrak{p}(\mathfrak{x}_1), w(\mathfrak{x} - \mathfrak{x}_2)\mathfrak{p}(\mathfrak{x}_2), ..., w(\mathfrak{x} - \mathfrak{x}_n)\mathfrak{p}(\mathfrak{x}_n) \right].$$

Furthermore, on solving Eq (5.2), the approximate solution is given by

$$y(\mathfrak{x}) \approx y_h(\mathfrak{x}) = \sum_{i=1}^{n} \Phi_i(\mathfrak{x})\mathbf{y}, \tag{5.3}$$

in which the MLS shape functions are obtained as

$$\Phi_i(\mathfrak{x}) = \begin{cases} \sum_{j=1}^{m} \mathfrak{p}_j(\mathfrak{x})\left(\mathbf{P}^{-1}(\mathfrak{x})\mathbf{S}(\mathfrak{x})\right)_{ji}, & \mathfrak{x} \in \mathfrak{d}_i, \\ 0, & \mathfrak{x} \notin \mathfrak{d}_i. \end{cases} \tag{5.4}$$

5.2. Node generation

Roos et al. [19] suggested that in the case of singularly perturbed problems, solutions possess rapid variations in some narrow regions adjacent to both the left and right lateral boundary when the singular perturbation parameter ϵ tends to 0. To capture these variations, we need to adopt some special adaptive techniques. In the present paper, we have utilized Shishkin's approach to generate more nodes in the boundary layer region and to capture these layers nicely. In Shishkin's approach, the distribution of nodes is carried out by dividing the spatial domain $\bar{\Omega} = [0, 1]$ into two subdomains $[0, \delta]$ and $[\delta, 1]$, where the transition parameter δ is chosen as

$$\delta = \min\{\frac{1}{2}, M\epsilon \ln N\},$$

where M is a constant chosen appropriately and $(N + 1)$ denotes the total number of nodes in the spatial domain. Here, we have considered that the boundary layers appear at $x = 0$ as $\epsilon \to 0$. Similar procedure can be carried out for boundary layers appearing at $x = 1$. Now, in each of these subdomains, the nodes are generated as follows:

$$x_i = \begin{cases} i * h_i, & i = 0, 1, ..., \frac{N}{2} \\ \delta + (i - N/2) * h_i, & i = \frac{N}{2} + 1, ..., N, \end{cases}$$

where the mesh spacings $h_i's$ are given by

$$h_i = \begin{cases} \frac{2\delta}{N}, & i = 0, 1, ..., \frac{N}{2} \\ \frac{2(1-\delta)}{N}, & i = \frac{N}{2} + 1, ..., N. \end{cases}$$

Remark. It is important to note that Shishkin's approach is only employed to generate nodes in this case, not the mesh, as the present method does not need elements or element connectivity.

5.3. Weak formulation

As discussed earlier in Section 4, in order to obtain the solution of the Fisher's problem, we consider its linear approximation (4.1), obtained by quasilinearization process.

The EFG weak formulation of linearized Eq (4.1) is mentioned as follows:

$$\frac{\epsilon\tau}{2}\int_{\Omega_x}\nabla y^{(n+1),(k+1)}\nabla\phi_i dx + [1 - \frac{\beta\tau}{2} + \beta\tau y^{(n+1),(k)}]\int_{\Omega_x} y^{(n+1),(k+1)}\phi_i dx - \delta\lambda(y - f(t))\Big|_{x=0} - \delta y\lambda\Big|_{x=0}$$

$$- \delta\rho(y - g(t))\Big|_{x=1} - \delta y\rho\Big|_{x=1} = (1 + \frac{\beta\tau}{2})\int_{\Omega_x} y^{(n)}\phi_i dx - \frac{\epsilon\tau}{2}\int_{\Omega_x}\nabla y^{(n)}\nabla\phi_i dx$$

$$- \frac{\beta\tau}{2}\int_{\Omega_x}(y^2)^{(n)}\phi_i dx + \frac{\beta\tau}{2}\int_{\Omega_x}(y^2)^{(n+1),(k)}\phi_i dx,$$

where ϕ_i's are the test functions formulated by MLS approach as specified in Section 5.1. The last terms on the left-hand side of the above equation are introduced due to the method of Lagrange multipliers to enforce the essential boundary conditions (1.3). By solving the above nodal weak formulations and assembling them, the resulted algebraic linear equations can be written in the matrix form as

$$\begin{bmatrix} K & G & H \\ G^T & 0 & 0 \\ H^T & 0 & 0 \end{bmatrix}\begin{bmatrix} Y \\ \lambda \\ \rho \end{bmatrix} = \begin{bmatrix} F \\ q \\ q_c \end{bmatrix},$$

where

$$K_{ij} = \epsilon\frac{\tau}{2}\int_{\Omega_x}\nabla\phi_j\nabla\phi_i dx + [1 - \beta\frac{\tau}{2} + \beta\tau\phi_j]\int_{\Omega_x}\phi_j\phi_i dx,$$

$$G_{lj}^T = -\delta\lambda_l(N_l\phi_j)\Big|_{x=0},$$

$$H_{lj}^T = -\delta\rho_l(R_l\phi_j)\Big|_{x=1},$$

$$F_i = (1 + \beta\frac{\tau}{2})\int_{\Omega_x} y^{(n)}\phi_i dx - \epsilon\frac{\tau}{2}\int_{\Omega_x}\nabla y^{(n)}\nabla\phi_i dx - \beta\frac{\tau}{2}\int_{\Omega_x}(y^2)^{(n)}\phi_i dx$$

$$+ \beta\frac{\tau}{2}\int_{\Omega_x}(y^2)^{(n+1),(k)}\phi_i dx,$$

$$q_l = -\delta\lambda_l(N_l f(t))\Big|_{x=0},$$

$$q_{c_l} = -\delta\rho_l(R_l g(t))\Big|_{x=1}.$$

Here, $\lambda = \sum_{l=1}^{n} N_l\lambda_l$ and $\rho = \sum_{l=1}^{n} R_l\rho_l$ are Lagrange multipliers and N_l and R_l are shape functions for l^{th} node on the essential boundary.

6. Numerical results and discussions

In this section, we will validate the theoretical findings and numerically demonstrate the consistency and accuracy of the proposed method with the help of examples. The L_∞-errors have been presented

for the considered problems. These errors have been estimated by

$$e_\epsilon^{N,\tau} = |\widehat{y}(x_i, t_j) - y(x_i, t_j)| \text{ and } E_\epsilon^{N,\tau} = \max_{i,j} e_\epsilon^{N,\tau},$$

where N symbolize number of nodes in the spatial direction, $t_j = j\tau$. Herein, $\widehat{y}(x,t)$ and $y(x,t)$ are exact and computed solutions respectively.

The order of convergence has been calculated by employing double mesh principle defined by

$$p_\epsilon^{N,\tau} = \left| \frac{\ln(E_\epsilon^{N,\tau}) - \ln(E_\epsilon^{2N,\tau/2})}{\ln(2)} \right|.$$

Example 6.1. *Consider the singularly perturbed nonlinear Fisher equation*

$$\frac{\partial y}{\partial t} = \epsilon \frac{\partial^2 y}{\partial x^2} + 6y(1 - y), \tag{6.1}$$

with initial condition

$$y(x, 0) = \frac{1}{(1 + e^{x/\sqrt{\epsilon}})^2},$$

and boundary conditions

$$y(0, t) = \frac{1}{(1 + e^{-5t})^2}, \quad y(1, t) = \frac{1}{(1 + e^{1/\sqrt{\epsilon}-5t})^2}.$$

*The exact solution of the considered problem is derived and is given by*

$$y(x, t) = \frac{1}{(1 + e^{x/\sqrt{\epsilon}-5t})^2}.$$

Based on the literature review, to the best of the Authors' knowledge, the problem under study has not yet been solved for small values of ϵ; hence no numerical results are available in the literature. The problem has been solved using the element-free Galerkin technique presented in the previous section for various values of the singular perturbation parameter ϵ and different numbers of nodes N.

Table 1 presents maximum error norm and rate of convergence of solution of Example 6.1 using the EFG method. The table depicts the numerical convergence of the proposed scheme. Figure 1 illustrates the mesh validation of the code for $\epsilon = 10^{-6}$ at time level $t = 1$. This graphical layout clearly demonstrates that even a grid of 32 nodes is sufficient enough to capture very sharp boundary layers occurring in the solution plot due to very small values of ϵ like 10^{-6}. Here the authors have employed Shishkin's approach to generating more nodes in the boundary layer region. For clear transparency, an expanded image has been presented for the boundary layer region. The effect of singular perturbation parameter, ϵ, on the EFG solutions have been displayed in Figure 2 for $N = 64$, $t = 0.5$ and for different values of ϵ. The boundary layers become sharper and sharper as $\epsilon \to 0$, and the proposed numerical approach efficiently captures these sharp layers in the solution as spectacled in the zoomed image for clarity.

Table 1. Maximum absolute errors and order of convergence in Example 6.1 for different values of ϵ at $t = 1.0$.

| ϵ	$N = 32$	$N = 64$	$N = 128$	$N = 256$
10^{-2}	9.65×10^{-3}	2.33×10^{-3}	5.78×10^{-4}	3.49×10^{-4}
	2.051	2.012	0.728	
10^{-3}	5.06×10^{-2}	1.55×10^{-2}	5.01×10^{-3}	1.61×10^{-3}
	1.707	1.630	1.637	
10^{-4}	5.06×10^{-2}	1.55×10^{-2}	5.01×10^{-3}	1.61×10^{-3}
	1.707	1.630	1.637	
10^{-5}	5.06×10^{-2}	1.55×10^{-2}	5.01×10^{-3}	1.61×10^{-3}
	1.707	1.630	1.637	
.	.	.	.	.
.	.	.	.	.
.	.	.	.	.
10^{-13}	5.06×10^{-2}	1.55×10^{-2}	5.01×10^{-3}	1.61×10^{-3}
	1.707	1.630	1.637	
10^{-14}	5.06×10^{-2}	1.55×10^{-2}	5.01×10^{-3}	1.61×10^{-3}
	1.707	1.630	1.637	
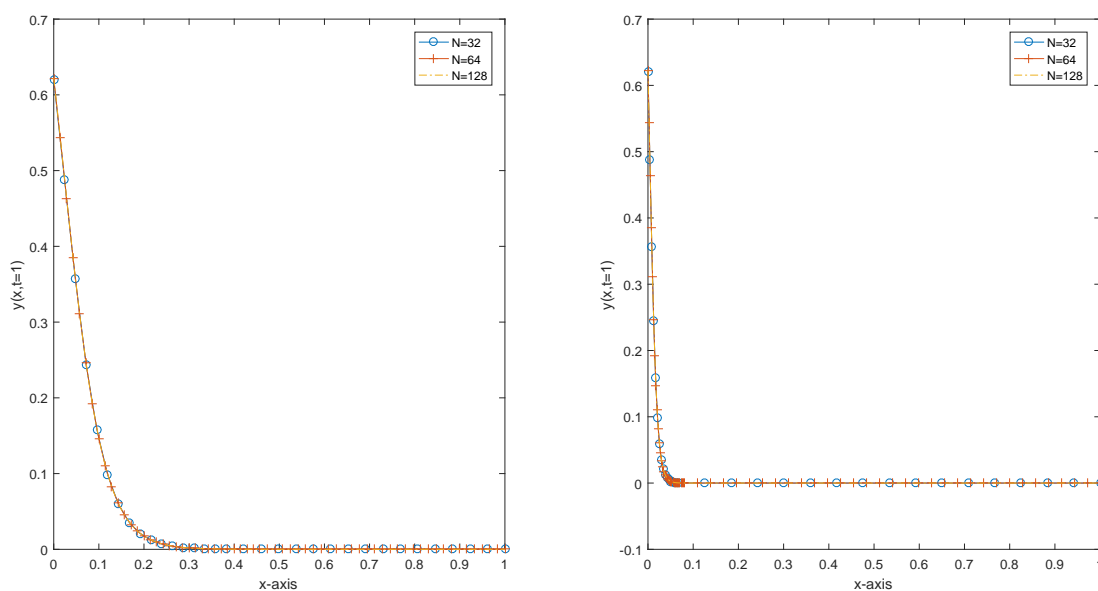
Figure 1. Grid validation for $\epsilon = 10^{-6}$ at $t = 1$.
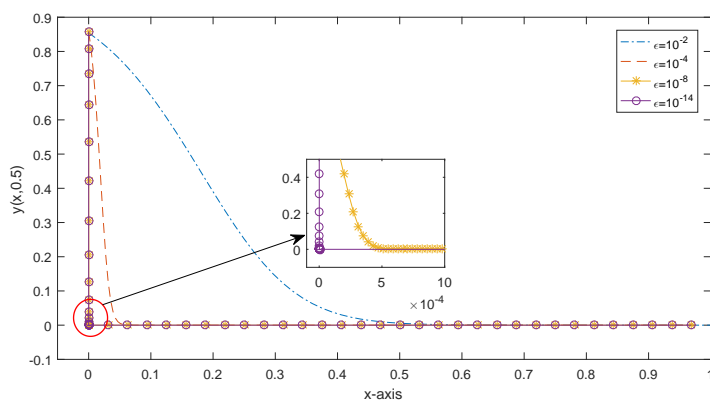
Figure 2. Epsilon-effect for $N = 64$ at $t = 0.5$.

In Figure 3, the solution has been plotted for $\epsilon=10^{-4}$, $N=32$ at different time levels $t=0.2, 0.4, 0.6, 0.8, 1.0$. The figure clearly justifies the capabilities of the proposed method in capturing the boundary layers in the solution at various time levels.
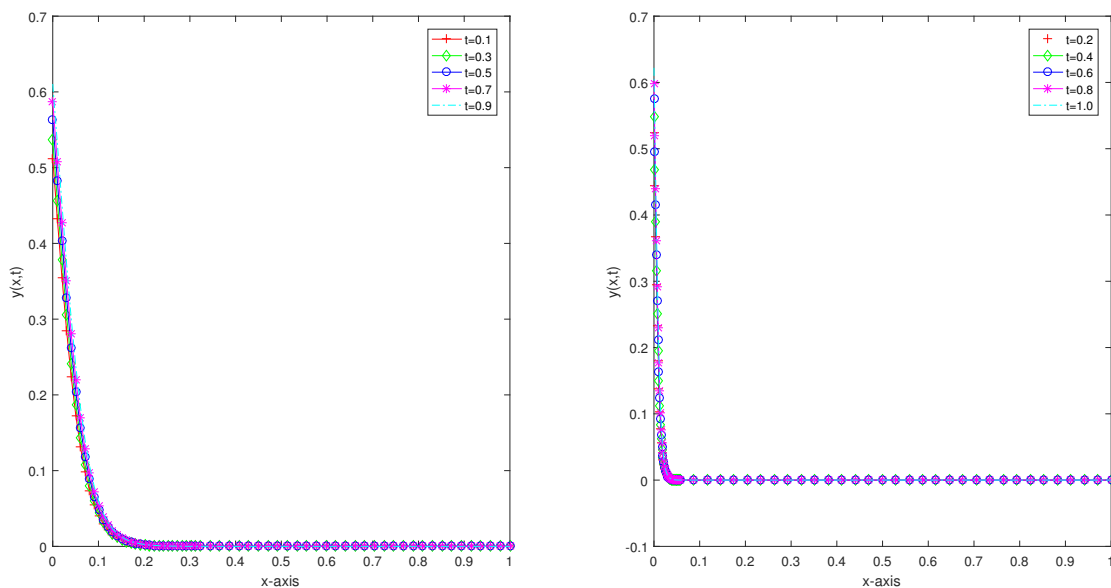

Figure 3. Time effect for $N = 32$ and $\epsilon = 10^{-4}$.

The comparison of the computed solutions with exact ones has been presented in Figure 4 for $N = 64$, $t = 1$ and $\epsilon = 10^{-2}$, 10^{-5}, 10^{-14}. The solution plots depict the efficiency and robustness of the proposed method. It can be observed that the plot of EFG solutions undoubtedly overlaps the plot of exact solutions.
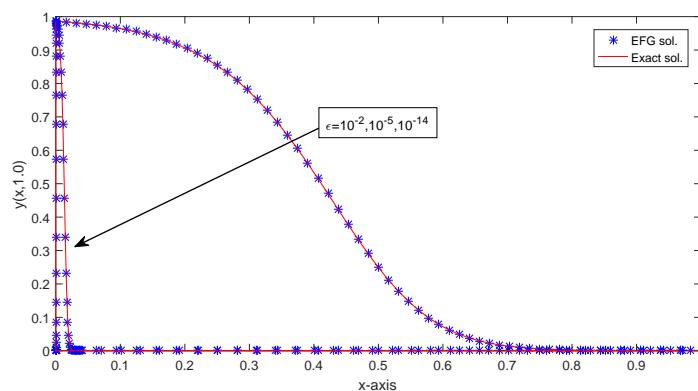
Figure 4. Exact and EFG solution plot for $N = 64$, $\epsilon = 10^{-2}$, 10^{-5}, 10^{-14} at $t = 1.0$.

The space-time evolution of the EFG solution profile has been shown in Figures 5 and 6 for $\epsilon = 10^{-2}$ and $\epsilon = 10^{-7}$ respectively. One can clearly observe how the EFG solution evolves as time increases. Also, the sharpness of the boundary layers can clearly be noticed. In the quasilinearization process, the scheme achieves the desired accuracy within four to five iterations at each time level.
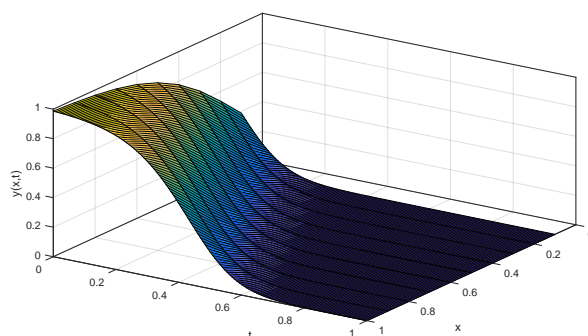
Figure 5. Evaluation of EFGM solution w.r.t. time for $\epsilon = 10^{-2}$.
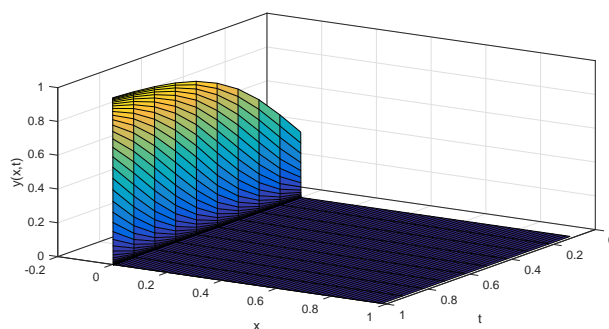
Figure 6. Evaluation of EFGM solution w.r.t. time for $\epsilon = 10^{-7}$.

Example 6.2. *For the second example, we have considered the following singularly perturbed*

nonlinear Fisher equation

$$\frac{\partial y}{\partial t} = \epsilon \frac{\partial^2 y}{\partial x^2} + u(1 - u^6),$$ (6.2)

with initial condition

$$y(x, 0) = \left[\frac{1}{2} + \frac{1}{2} \tanh\left(\frac{-3x}{4\epsilon}\right)\right]^{1/3},$$

and boundary conditions

$$y(0, t) = \left[\frac{1}{2} + \frac{1}{2} \tanh\left(\frac{15t}{8}\right)\right]^{1/3}, \quad y(1, t) = \left[\frac{1}{2} + \frac{1}{2} \tanh\left(\frac{-3}{4\epsilon} + \frac{15t}{8}\right)\right]^{1/3}.$$

The boundary layers for the problem under consideration occur at both boundary points, i.e., at $x = 0$ and $x = 1$. To the best of the Authors' knowledge, this problem has not yet been solved in literature for small values of the singular perturbation parameter ϵ. Here the problem has been solved by using the EFG method to check the convergence and robustness of the proposed method.

Table 2 provides the maximum norm errors and rate of convergence obtained for Example 6.2. In this table, the time level is fixed at $t = 1.0$, and the number of nodes changes. The outcomes clearly depict the parameter uniform numerical convergence of the proposed method as $\epsilon \to 0$.

Table 2. Maximum absolute errors and rate of convergence in Example 6.2 for different values of ϵ at $t = 1.0$.

| ϵ	$N = 32$	$N = 64$	$N = 128$	$N = 256$
2^{-2}	1.83×10^{-2}	1.51×10^{-2}	1.61×10^{-3}	1.29×10^{-3}
	0.277	3.229	0.319	
2^{-4}	2.88×10^{-2}	1.18×10^{-2}	4.06×10^{-3}	1.51×10^{-3}
	1.280	2.744	1.426	
2^{-6}	3.12×10^{-2}	4.07×10^{-3}	4.02×10^{-4}	4.56×10^{-5}
	2.938	3.339	3.140	
2^{-8}	3.17×10^{-2}	4.07×10^{-3}	3.60×10^{-4}	2.86×10^{-5}
	2.961	3.498	3.654	
2^{-10}	3.38×10^{-2}	4.03×10^{-3}	3.27×10^{-4}	3.34×10^{-5}
	3.068	3.623	3.291	
2^{-12}	3.37×10^{-2}	4.01×10^{-3}	3.26×10^{-4}	2.90×10^{-5}
	3.071	3.620	3.490	
2^{-14}	3.37×10^{-2}	4.04×10^{-3}	3.26×10^{-4}	2.91×10^{-5}
	3.061	3.631	3.486	
2^{-16}	3.36×10^{-2}	4.04×10^{-3}	3.26×10^{-4}	2.91×10^{-5}
	3.061	3.631	3.486	
2^{-18}	3.36×10^{-2}	4.04×10^{-3}	3.26×10^{-4}	2.91×10^{-5}
	3.061	3.631	3.486	
2^{-20}	3.36×10^{-2}	4.04×10^{-3}	3.26×10^{-4}	2.91×10^{-5}
	3.061	3.631	3.486	

The physical behavior of the solution has been shown in Figures 7–10 for different values of the parameters.

Figure 7 illustrates the singular purturbation parameter ϵ-effect on the EFG solution for various values of $\epsilon = 2^{-2}$, 2^{-4}, 2^{-8}, 2^{-16}, 2^{-20} at $t = 0.9$ and for $N = 64$. The evolution of sharp boundary layers at both the endpoints of the domain has clearly been observed and highlighted through the zoomed figure, as ϵ tends to zero.
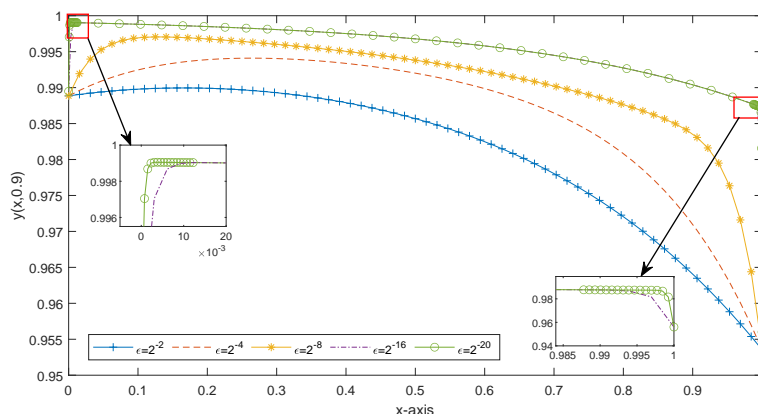

Figure 7. Epsilon-effect for $N = 64$ at $t = 0.9$.

The impact of different time levels $t = 0.1$, 0.3, 0.5, 0.7, 0.9 on the EFG solution for $N = 64$ and $\epsilon = 2^{-13}$ has been presented in Figure 8. The proficiency of the proposed method in capturing edgy boundary layers at various time levels is easily verified through these plots.
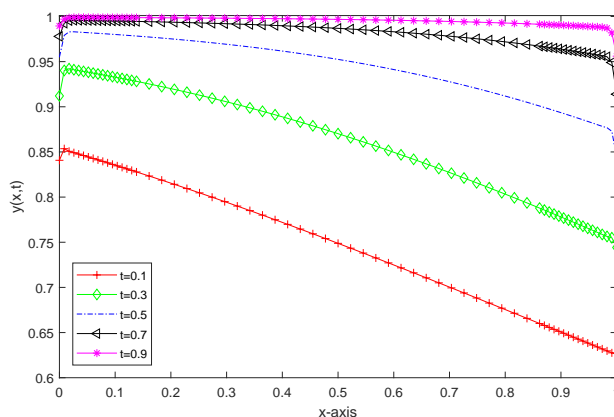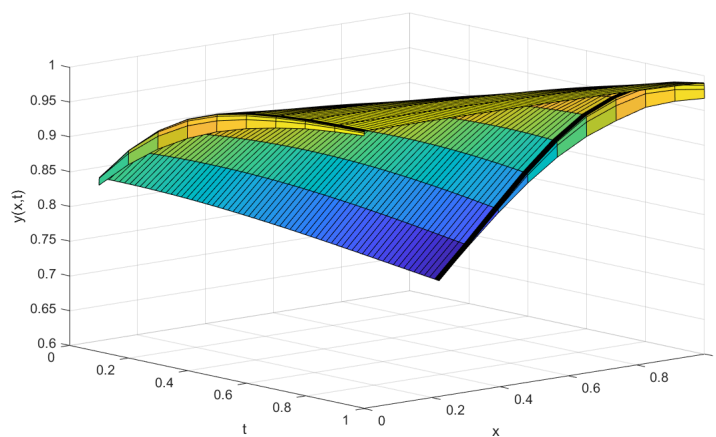

Figure 8. Time effect for $N = 64$ and $\epsilon = 2^{-13}$.

The three-dimensional visualization of element-free Galerkin solution with respect to time-space profile have been represented through Figures 9 and 10 for $\epsilon = 2^{-2}$ and $\epsilon = 2^{-20}$ respectively.
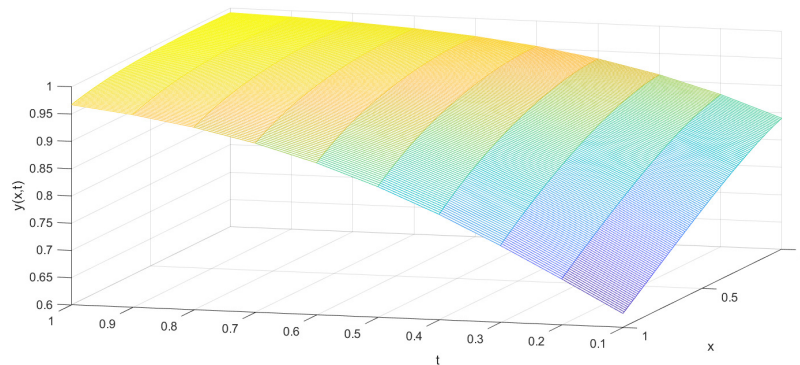
Figure 9. Evaluation of EFGM solution w.r.t. time for $\epsilon = 2^{-2}$.

Figure 10. Evaluation of EFGM solution w.r.t. time for $\epsilon = 2^{-20}$.

7. Conclusions

In the present work, the element-free Galerkin method along with the Crank-Nicolson technique has been proposed for the singularly perturbed Fisher equation. The semi-discrete scheme is unconditionally stable in the energy norm with second-order convergence. The nonlinearity present in the problem has been handled by utilizing the quasilinearization approach, and its rate of convergence has also been studied. To capture the sharp boundary layers more precisely, non-uniformly distributed grid points condensing near the boundary layers have been generated. Two numerical examples have been considered to validate the theoretical results. The numerical results depict the robustness and efficiency of the proposed scheme in capturing very sharp boundary layers even for a significantly less number of nodes and hence proving the computational efficiency of the method. Overall, the author's found that the proposed scheme provides satisfactory results for approximating the solution of the non-linear Fisher's problem. Also, the problems under consideration have not yet been solved in the literature to the best of the author's knowledge for the small value of the singular perturbation parameter. It will be interesting to verify the proposed method for fractional order singularly perturbed differential equations.

Acknowledgments

Conflict of interest

The authors declare no conflicts of interest in the present work.

References

1. M. Ablowitz, A. Zeppetella, Explicit solutions of Fisher's equation for a special wave speed, *Bltn. Mathcal. Biology*, **41** (1979), 835–840. http://dx.doi.org/10.1007/BF02462380

2. K. Al-Khaled, Numerical study of Fisher's reaction-diffusion equation by the sinc collocation method, *J. Comput. Appl. Math.*, **137** (2001), 245–255. http://dx.doi.org/10.1016/S0377-0427(01)00356-9

3. A. Atangana, On the new fractional derivative and application to nonlinear Fisher's reaction-diffusion equation, *Appl. Math. Comput.*, **273** (2016), 948–956. http://dx.doi.org/10.1016/j.amc.2015.10.021

4. L. Balyan, A. Mittal, M. Kumar, M. Choube, Stability analysis and highly accurate numerical approximation of Fisher's equations using pseudospectral method, *Math. Comput. Simulat.*, **177** (2020), 86–104. http://dx.doi.org/10.1016/j.matcom.2020.04.012

5. I. Grant, Quasilinearization and non-linear boundary value problems by R. E. Bellman and R. E. Kalaba (1965), *Math. Gaz.*, **52** (1968), 212–212. http://dx.doi.org/10.2307/3612757

6. J. Canosa, Diffusion in nonlinear multiplicative media, *J. Math. Phys.*, **10** (1969), 1862. http://dx.doi.org/10.1063/1.1664771

7. G. Carey, Y. Shen, Least-squares finite element approximation of Fisher's reaction-diffusion equation, *Numer. Meth. Part. D. E.*, **11** (1995), 175–186. http://dx.doi.org/10.1002/num.1690110206

8. I. Dag, O. Ersoy, The exponential cubic b-spline algorithm for Fisher equation, *Chaos Soliton. Fract.*, **86** (2016), 101–106. http://dx.doi.org/10.1016/j.chaos.2016.02.031

9. Z. Feng, Y. Li, Complex traveling wave solutions to the Fisher equation, *Physica A*, **366** (2006), 115–123. http://dx.doi.org/10.1016/j.physa.2005.10.058

10. R. Fisher, The wave of advance of advantageous genes, *Annals of eugenics*, **7** (1937), 355–369. http://dx.doi.org/10.1111/j.1469-1809.1937.tb02153.x

11. P. Gray, S. Scott, *Chemical oscillations and instabilities: non-linear chemical kinetics*, Clarendon: Clarendon Press, 1990.

12. E. Infeld, G. Rowlands, *Nonlinear waves, solitons and chaos*, Cambridge: Cambridge university press, 2000.

13. M. Khader, K. Saad, A numerical approach for solving the fractional Fisher equation using chebyshev spectral collocation method, *Chaos Soliton. Fract.*, **110** (2018), 169–177. http://dx.doi.org/10.1016/j.chaos.2018.03.018

14. S. Kumar, R. Jiwari, R. Mittal, Radial basis functions based meshfree schemes for the simulation of non-linear extended Fisher-kolmogorov model, *Wave Motion*, **109** (2021), 102863. http://dx.doi.org/10.1016/j.wavemoti.2021.102863

15. X. Li, S. Li, A fast element-free galerkin method for the fractional diffusion-wave equation, *Appl. Math. Lett.*, **122** (2021), 107529. http://dx.doi.org/10.1016/j.aml.2021.107529

16. R. Mickens, A best finite-difference scheme for the Fisher equation, *Numer. Meth. Part. D. E.*, **10** (1994), 581–585. http://dx.doi.org/10.1002/num.1690100505

17. R. Mittal, R. Jiwari, Numerical study of Fisher's equation by using differential quadrature method, *Int. J. Inf. Syst. Sci.*, **5** (2009), 143–160.

18. D. Olmos, B. Shizgal, A pseudospectral method of solution of Fisher's equation, *J. Comput. Appl. Math.*, **193** (2006), 219–242. http://dx.doi.org/10.1016/j.cam.2005.06.028

19. H. Roos, M. Stynes, L. Tobiska, *Robust numerical methods for singularly perturbed differential equations: convection-diffusion-reaction and flow problems*, Berlin: Springer, 2008. http://dx.doi.org/10.1007/978-3-540-34467-4

20. M. Rosa, S. Chulián, M. Gandarias, R. Traciná, Application of lie point symmetries to the resolution of an interface problem in a generalized Fisher equation, *Physica D*, **405** (2020), 132411. http://dx.doi.org/10.1016/j.physd.2020.132411

21. S. Tang, R. Weber, Numerical study of Fisher's equation by a petrov-galerkin finite element method, *The ANZIAM Journal*, **33** (1991), 27–38. http://dx.doi.org/10.1017/S0334270000008602

22. J. Tyson, P. Brazhnik, On traveling wave solutions of Fisher's equation in two spatial dimensions, *SIAM J. Appl. Math.*, **60** (2000), 371–391. http://dx.doi.org/10.1137/S0036139997325497

23. M. Uzunca, B. Karasözen, T. Küçükseyhan, Moving mesh discontinuous Galerkin methods for PDEs with traveling waves, *Appl. Math. Comput.*, **292** (2017), 9–18. http://dx.doi.org/10.1016/j.amc.2016.07.034

24. X. Wang, Exact and explicit solitary wave solutions for the generalised Fisher equation, *Phys. Lett. A*, **131** (1988), 277–279. http://dx.doi.org/10.1016/0375-9601(88)90027-8

25. A. Wazwaz, A. Gorguis, An analytic study of Fisher's equation by using adomian decomposition method, *Appl. Math. Comput.*, **154** (2004), 609–620. http://dx.doi.org/10.1016/S0096-3003(03)00738-0

26. T. Zhang, X. Li, L. Xu, Error analysis of an implicit galerkin meshfree scheme for general second-order parabolic problems, *Appl. Numer. Math.*, **177** (2022), 58–78. http://dx.doi.org/10.1016/j.apnum.2022.03.005